



## Supplementary Materials for

### **Inhibition protects acquired song segments during vocal learning in zebra finches**

Daniela Vallentin, Georg Kosche, Dina Lipkind, Michael A. Long\*

\*Corresponding author. E-mail: [mlong@med.nyu.edu](mailto:mlong@med.nyu.edu)

Published 15 January 2016, *Science* **351**, 267 (2016)  
DOI: 10.1126/science.aad3023

**This PDF file includes:**

Materials and Methods

Figs. S1 to S10

Caption for movie S1

References

**Other supplementary material for this manuscript includes the following:**

Movie S1

## Materials and Methods

### Animals

All animal maintenance and experimental procedures were performed according to the guidelines established by the Institutional Animal Care and Use Committee at the New York University Langone Medical Center. For these experiments, male zebra finches were acquired from an outside breeding facility (Hunter College) and reared in the absence of adult males during the first postnatal month. Afterwards, birds were kept in sound attenuation chambers with either an adult male tutor (introduced after posthatch day 43) or a small speaker placed within the chamber beginning on posthatch day 33.

### Surgery

To enable electrophysiological recordings, zebra finches were first anesthetized with isoflurane (1–3% in oxygen) and a headplate was affixed to the skull using dental acrylic. In cases in which premotor neurons were targeted with sharp intracellular recordings, a bipolar stimulating electrode was inserted into the robust nucleus of the arcopallium (RA) in order to antidromically identify HVC neurons that project to that nucleus (34). For 2-photon targeted voltage-clamp recordings, premotor neurons were labeled with a 50 nL injection of a green fluorescent retrograde tracer (Lumafuor) into RA using an oil-based pressure injection system (Nanoject, Drummond). In those animals, we performed a craniotomy (1-2 mm diameter) directly above HVC, and dura was removed as well as a small region of the hippocampal formation overlying HVC. A thin cover glass (3 mm, #1 thickness, Warner Instruments) was then affixed to the skull using cyanoacrylate to create a chronic optical window.

### Electrophysiological recordings

Three recording methods (sharp intracellular, juxtacellular, and whole-cell) were used as part of this study. All membrane potential and current measurements were digitized at 40 kHz using a National Instruments acquisition board and acquired with custom MATLAB software.

*Sharp intracellular recordings:* On the day of recording (1–4 d after surgery), we prepared a small (200  $\mu\text{m}$  diameter) craniotomy above HVC and carefully removed overlying dura. A well was built around the craniotomy using a silicone elastomer (Kwik-Cast; WPI). To protect the brain from desiccation, the well was filled with either phosphate buffered saline (PBS) or a silicone gel (Dow Corning; 10,000–60,000 cSt) during recording sessions and with a layer of silicone elastomer overnight. Projection neurons were identified antidromically (34) using a bipolar stimulating electrode implanted into RA. A positive identification was associated with a reliable spike in HVC with minimal latency jitter ( $<50 \mu\text{s}$ ) evoked with single biphasic (200  $\mu\text{s}$  per phase) current pulses of  $<250 \mu\text{A}$ . Recording electrodes (borosilicate glass with filament, O.D.: 1.0 mm, I.D.: 0.5 mm) with an impedance of 70–130 M $\Omega$  were prepared using a horizontal micropipette puller (P-97; Sutter Instrument Company) and backfilled with 3 M potassium acetate. Zebra finches were head-fixed (without anesthesia) and partially immobilized in a foam restraint. The electrodes were lowered into HVC in  $\sim 5 \mu\text{m}$  steps using a micromanipulator (MP-285, Sutter Instruments). A brief (10–20 ms) 'buzz' pulse was often needed to facilitate the penetration of the membrane. Acceptable recordings were defined as having a spike height greater than 40 mV, a resting membrane potential of at least  $-50 \text{ mV}$ , and a total recording duration greater than 3 minutes.

*Juxtacellular recordings of HVC interneurons or RA neurons:* Recording sessions commenced at least one day following surgery. Juxtacellular pipettes (borosilicate glass with filament, O.D.: 1.5 mm, I.D.: 0.86 mm, Sutter Instrument Company) with an impedance of 3–10 M $\Omega$  were pulled using a horizontal micropipette puller (P-97, Sutter Instrument Company) and filled with 0.5 M sodium chloride. Zebra finches were head-fixed, and electrodes were lowered into HVC or RA. Acceptable recordings were defined as having a signal-to-noise ratio greater than 5.

*2-photon targeted whole-cell recordings:* On the day of recording, a small hole (~100  $\mu$ m diameter) was carefully drilled into the implanted cover slip using a carbide bur (0.3 mm diameter) just lateral to the visually determined center of HVC. The bird was given at least another two hours of recovery time after this procedure to ensure that any effects of isoflurane anesthesia had subsided. For every day of recording, a new hole was drilled to gain access to previously unrecorded region of HVC. After the recovery period, the zebra finch was placed in a foam restraint and head-fixed under a customized moveable objective 2-photon microscope (Sutter Instrument Company). Premotor neurons (labeled with green retrobeads) were imaged using a Ti:Sapphire laser (Coherent Chameleon) tuned to 800 nm. Fluorescent light was gathered through a 25X water immersion objective (Olympus) and detected using a GaAsP photomultiplier tube (H10770PA-40 PMT Module, Hamamatsu). Images were captured using Scanimage 3.8 (35). Whole-cell patch pipettes were pulled from borosilicate glass with filament (O.D.: 1.5 mm, I.D.: 0.86 mm) using a P-97 micropipette puller (Sutter Instrument Company) and filled with voltage-clamp internal solution (in mM: CsMeS [130], CsCl [4], NaCl [2], HEPES [10], EGTA [0.2], phosphocreatine-Tris [14], QX-314 [5], ATP-Mg [4], GTP-Tris [0.3]) containing 25  $\mu$ M Alexa Fluor 594 (Life Technologies) to gain a final tip resistance of 4-6 M $\Omega$ . A physiological buffering solution (in mM: NaCl [125], KCl [5], D-(+)-glucose [10], HEPES [10], CaCl<sub>2</sub> [2], MgSO<sub>4</sub> [2]) was added on top of the cranial window, and pipettes were lowered through the hole in the cranial window using a motorized micromanipulator MP-285 (Sutter Instrument Company) under 2.0 PSI of positive pressure. Once pipettes penetrated into HVC, positive pressure was reduced to 0.25 PSI. With the red dye in the pipette filling the extracellular space, previously described techniques (36, 37) were used to target premotor neurons visibly containing green retrobeads. Upon visual contact with the membrane, positive pressure was released and a G $\Omega$  seal was formed. Slow and fast pipette capacitances were compensated, and whole-cell access was gained by applying a negative pulse of pressure. Recordings were done using a Multiclamp 700B amplifier digitized at 40 KHz. Access and input resistance were monitored at the beginning of each recording and with each change of recording configuration. A -14 mV liquid junction potential was corrected in all voltage-clamp recordings. Cells were clamped either at -68 mV (to measure excitation) or 0 mV (to measure inhibition). After a recording was completed, images were captured of the recorded neuron. Acceptable recordings were defined as having access resistances less than 50 M $\Omega$ .

*Pharmacological manipulation:* In some experiments, the GABA<sub>A</sub> antagonist gabazine was unilaterally applied to HVC in the adult zebra finch. Because HVC is a superficial structure, we introduced gabazine (0.01–0.1 mM in saline) into the well surrounding our craniotomy, and recordings proceeded as previously described. The small craniotomy size (< 200  $\mu$ m diameter) was intended to help restrict the spread of gabazine.

## Sound recording and tutor song presentation

All sounds were recorded using an omnidirectional lavalier microphone (AT 803b; Audio-Technica) and amplified using a PreSonus Studio Channel amplifier. Audio recordings were digitized at 20 kHz using a National Instruments board. The songs produced in the behavioral observation boxes were recorded using a Focusrite Saffire Pro 40 and digitized at 44.1 kHz. Sound Analysis Pro 2011 (38) was used to extract song recordings recorded in the home cages. The tutor song was presented during electrophysiological recordings using USB powered speakers (Altec Lansing BXR 1220). The sound level was calibrated to 70-80 dB sound pressure level (SPL) using a digital SPL meter (Nady Audio DSM-1). The minimal time allowed between tutor song presentations was three seconds. All birds were visually monitored to ensure that they were not sleeping during recordings.

## Data Analysis

We used MATLAB (MathWorks, Inc., Natick, MA) for data analysis. All data are presented as *mean ± SD*.

*Spiking analysis:* The song playback and the accompanying spiking activity were aligned by detecting the onset and the offset of each playback and warping the electrophysiological trace linearly across trials. Spikes were extracted using a thresholding algorithm. The firing rate change is defined as

$$\Delta \text{ firing rate} = \frac{\text{firing rate (tutor)} - \text{firing rate (silence)}}{\text{firing rate (tutor)} + \text{firing rate (silence)}}$$

We defined ‘silence’ as the 1000 ms period preceding the tutor song playback and ‘tutor’ as a time window that encompasses the duration of the tutor song plus 50 ms to account for the time needed for auditory responses to impact HVC (39).

*Spiking precision:* For every spike  $\in$  [tutor<sub>ikx</sub>(start)+20 ms, tutor<sub>ikx</sub>(end)+30 ms] in trial i of neuron k in bird x, the latency to every other spike  $\in$   $\cup_{j \neq i} [\text{tutor}_{jkx}(\text{start}), \text{tutor}_{jkx}(\text{end})+50 \text{ ms}]$  in all the other trials in neuron k (except trial i) was determined. This resulted in a distribution of latencies. We extracted the number of latencies in a  $\pm 20$  ms window (L20) and normalized it by dividing L20 by the number of all latencies (NL20). We shuffled the data 1000 times randomly choosing from the distribution of firing rates for each neuron and calculated the NL20 for the shuffled data, resulting in a distribution of 1000 ‘shuffled NL20s’. A z-score was calculated:

$$\text{z-score(NL20)} = \frac{\text{NL20} - \text{mean}(\text{shuffled NL20s})}{\text{std}(\text{shuffled NL20s})}$$

Precision was then defined as:

$$\text{precision (tutor)} = \text{sign}(\text{z-score (NL20)}) \times \sqrt{(|\text{z-score(NL20)}|)}$$

This analysis was applied in the same way to the spikes recorded during silence for every spike  $\in$  [silence<sub>ikx</sub>(start)+20 ms, silence<sub>ikx</sub>(end)] resulting in the following definition of precision during silence:

$$\text{precision (silence)} = \text{sign}(\text{z-score (NL20}_{\text{silence}})) \times \sqrt{(|\text{z-score}(\text{NL20}_{\text{silence}})|)}.$$

*Subthreshold variance:* From the tutor song-aligned membrane potential, the mean value was subtracted. A thresholding algorithm detected and removed the spikes ( $\pm 3$  ms) and the subsequent gap was linearly interpolated. From the resulting subthreshold membrane potential the variance during tutor song playback was calculated.

*Subthreshold precision:* To analyze the similarity of recorded traces, we performed a pairwise cross-correlation on subthreshold membrane potential activity (spikes were removed as described above) during tutor song playback. The 95% confidence interval (mean value  $\pm 1.96 \times \text{SEM}$ ) was extracted from the cross-correlation values of the silence.

*Event detection (voltage clamp recordings):* The current traces were Savitzky-Golay filtered (2<sup>nd</sup> polynomial degree with 1.75 ms resolution). For inhibitory currents local peaks whose amplitude exceeded 35 pA were detected with a customized local maxima detection algorithm (fig. S2). The corresponding onset was detected within a 7 ms window prior to the peaks. The amplitude and frequency of these events during silence and tutor song playback was determined and shown as amplitude distributions. The tutor song evoked events were calculated as the difference between silence and playback amplitude distributions. The same algorithm was applied to the excitatory current trace (amplitude  $\geq 20$ -25 pA, 4.75-7 ms window) once we had inverted the signal by multiplying by -1.

*Synaptic changes:* To quantify synaptic changes we defined the following indices:

$$\Delta \text{ charge} = \frac{\text{charge (tutor)} - \text{charge (silence)}}{\text{charge(tutor)} + \text{charge (silence)}}$$

$$\Delta \text{ amplitude} = \frac{\text{amplitude (tutor)} - \text{amplitude (silence)}}{\text{amplitude(tutor)} + \text{amplitude (silence)}}$$

$$\Delta \text{ frequency} = \frac{\text{frequency (tutor)} - \text{frequency (silence)}}{\text{frequency(tutor)} + \text{frequency (silence)}}$$

Charge was defined as the absolute area under the curve (inhibitory current trace or negative excitatory current trace) with respect to 0 pA. Amplitude was calculated as the difference between the measured current at the time of a detected peak and the corresponding onset. The frequency was defined as the number of all detected peaks per second. For voltage clamp recordings we chose the first 750 ms of the 1 sec period preceding the tutor song playback as ‘silence’ and the duration of the tutor song plus 50 ms as ‘tutor’.

*Synaptic precision (current recordings):* The current traces were Savitzky-Golay filtered (2<sup>nd</sup> polynomial degree with 1.75 ms resolution). The mean value was subtracted from each trace. We performed a pair wise cross-correlation on excitatory or inhibitory current recordings during tutor song playback. The 95% confidence interval (mean value  $\pm 1.96 \times \text{SEM}$ ) was extracted from the cross-correlation values of the silence.

*Across-cell precision:* In cases where more than one cell per bird was recorded, all the recordings of excitatory or inhibitory currents were pooled. A pairwise cross-correlation on the pooled excitatory or inhibitory current recordings during tutor song playback was performed.

*% firing during a specific syllable:* The baseline firing rate (baseline) of interneurons was calculated as the mean firing rate during the silence period (1000 ms preceding tutor song start). To identify the parts of the tutor song playback that evoked a significant increase in interneuron firing  $1.96 \times \text{SD}$  was added to the baseline and set as a threshold. The duration that the PSTH positively crossed this threshold for at least 5 ms was considered to be the time when interneuron activity was significantly increased. These time intervals were then assigned to the corresponding syllables and the duration that syllable A or B is covered with significant interneuron firing rate was determined. This extracted duration of significant activity was related to the entire duration of both syllable A's (or B's) and expresses as a percentage.

*% inhibition during a specific syllable:* The same algorithm as for % firing during a specific syllable was applied to the average recorded current trace during ABAB playback. The baseline was extracted from the first 750 ms of the 1000 ms preceding tutor song playback.

*Song similarity:* For quantification of song performance, spectral features of the song were measured to calculate the degree of similarity to the tutor song (SAP 2011) (38). Briefly, we obtained two different measures of song similarity: (1) “% local similarity” measures the percentage of a song that is considered to be similar (based on 50 ms intervals) to the song it is compared with and (2) “accuracy” measures the local similarity of sections on a 1 ms timescale. To establish a conservative measure of song similarity we first calculated % similarity(control) = % local similarity  $\times$  accuracy for control birds where we compared 5-10 different renditions of an adult bird's own song (BOS). The similarity of a bird's own song to its tutor song was then calculated as

$$\% \text{ similarity to tutor song} = \frac{\% \text{ local similarity (BOS vs tutor)} \times \text{accuracy (BOS vs.tutor)}}{\% \text{ similarity (control)}}$$

SAP 2011 considers acoustic features such as pitch, goodness of pitch, frequency and amplitude modulation, and Wiener entropy between song motifs to provide a statistical estimate of overall similarity. We used the SAP 2011 default settings that are optimized for zebra finch song:  $p = 0.05$ , interval = 70 ms; minimum duration = 15 ms applied on the entire song. For scoring similarity, we used the asymmetric and mean value settings for motif comparisons and symmetric and mean value settings for syllable by syllable comparisons. For each bird, we compared 6–10 songs (8-12 syllables).

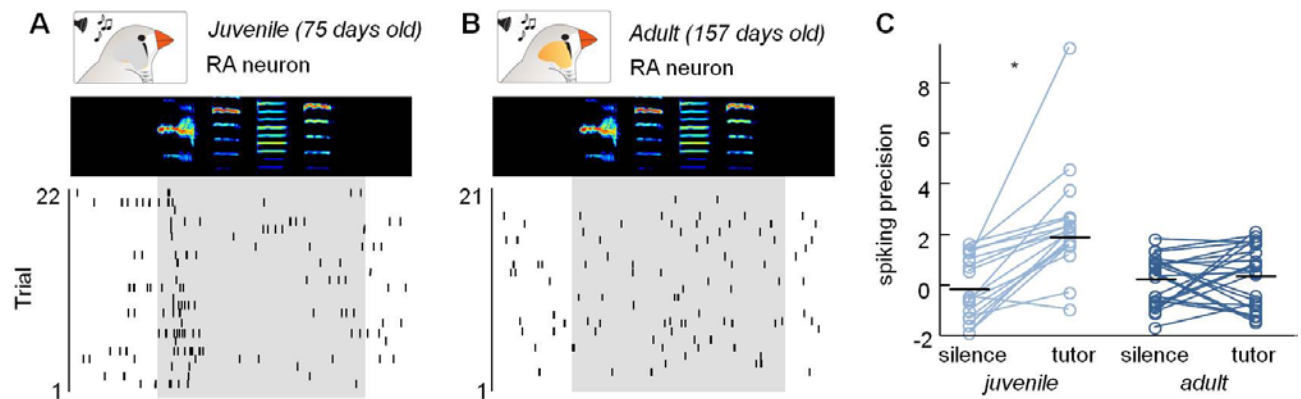
*Statistics:* To test for significant differences, we had to take the nested structure of the data into account because multiple neurons were often recorded in the same animal. In cases when we recorded paired data, we used a repeated measures ANOVA and reported only the main effect. For metrics that could be measured in individual trials (firing rate), we analyzed the data for each trial, controlling for neuronal identity in order to account for any variability in the number of trials for each neuron. In metrics that measured properties across trials (precision), we analyzed the summary parameters for each neuron, controlling for bird identity. For unpaired data (variance, subthreshold precision, precision of interneuron firing rate) we used the non parametric Wilcoxon rank sum test. In order to account for the nested structure (neurons within

birds) in continuous data, we fitted a linear mixed model by maximum likelihood estimation (changes in interneuron firing depending on similarity; changes in inhibition and excitation depending on age or similarity). We used the following model specifications:

dependent variable  $\sim$  1 + independent variable + (1 + independent variable | bird identity)

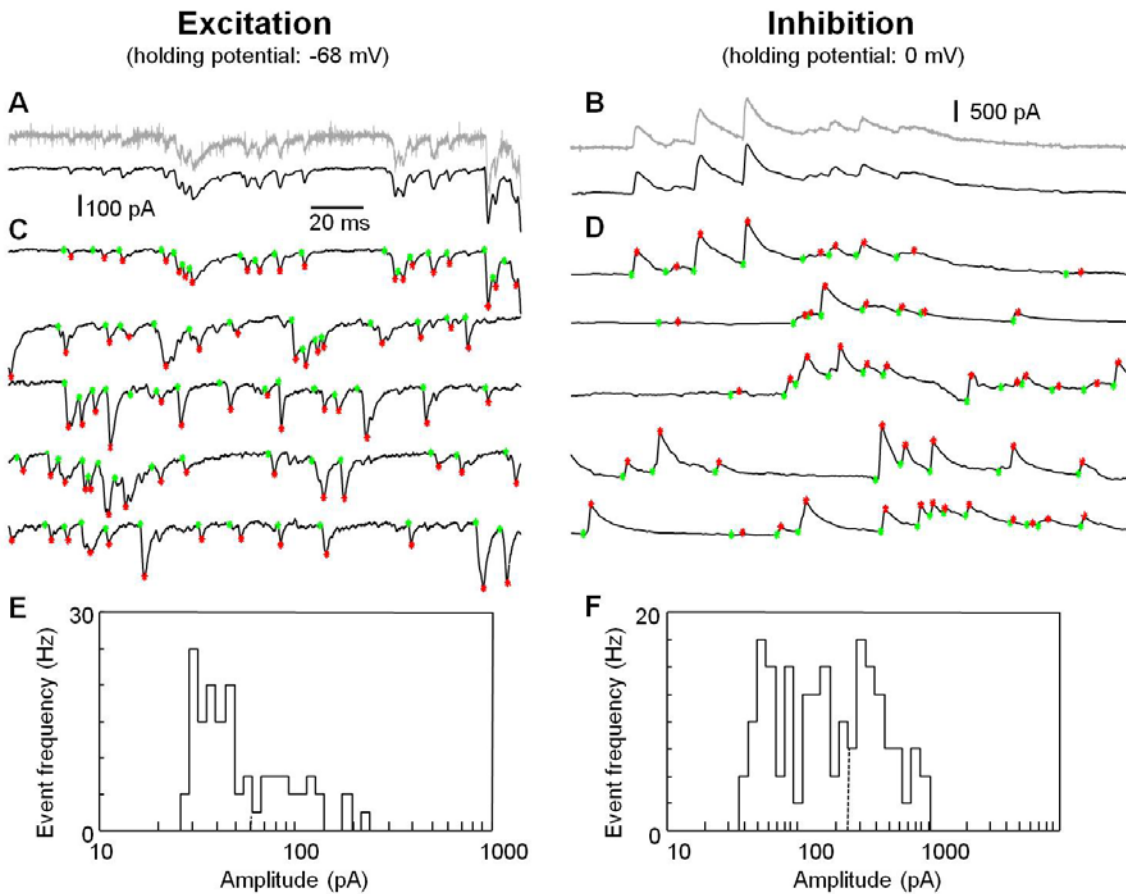
## Figures S1-S10

Fig. S1



**Fig. S1. Tutor song can evoke spiking responses in RA neurons of juvenile but not adult zebra finches.** (A and B) Raster plots of tutor-song evoked spiking in RA neurons recorded in a juvenile (A) and an adult (B) during tutor song presentation. Data were collected from same the birds shown in Figs. 1A and 1D respectively. (C) Spiking precision during silence versus the tutor song in the juvenile (silence:  $-0.1 \pm 1.2$ , tutor:  $2.4 \pm 2.1$ ,  $P = 0.016$ , repeated measures ANOVA) and the adult (silence:  $0.1 \pm 1.0$ , tutor:  $0.4 \pm 1.2$ ;  $P = 0.66$ , repeated measures ANOVA).

**Fig. S2**



**Fig. S2. Detection of excitatory and inhibitory synaptic events.** (A and B) Raw voltage-clamp recording from an HVC premotor neuron showing excitatory (A) and inhibitory (B) currents. Unfiltered (gray) and filtered (black) traces are provided (see Methods for details). (C and D) Five example excitatory (C) and inhibitory (D) current traces from a single HVC premotor neuron. Event onsets (green asterisks) and extrema (red asterisks) are indicated. (E and F) Amplitude histograms showing the excitatory (E) and inhibitory (F) events detected in the above traces.

**Fig. S3**

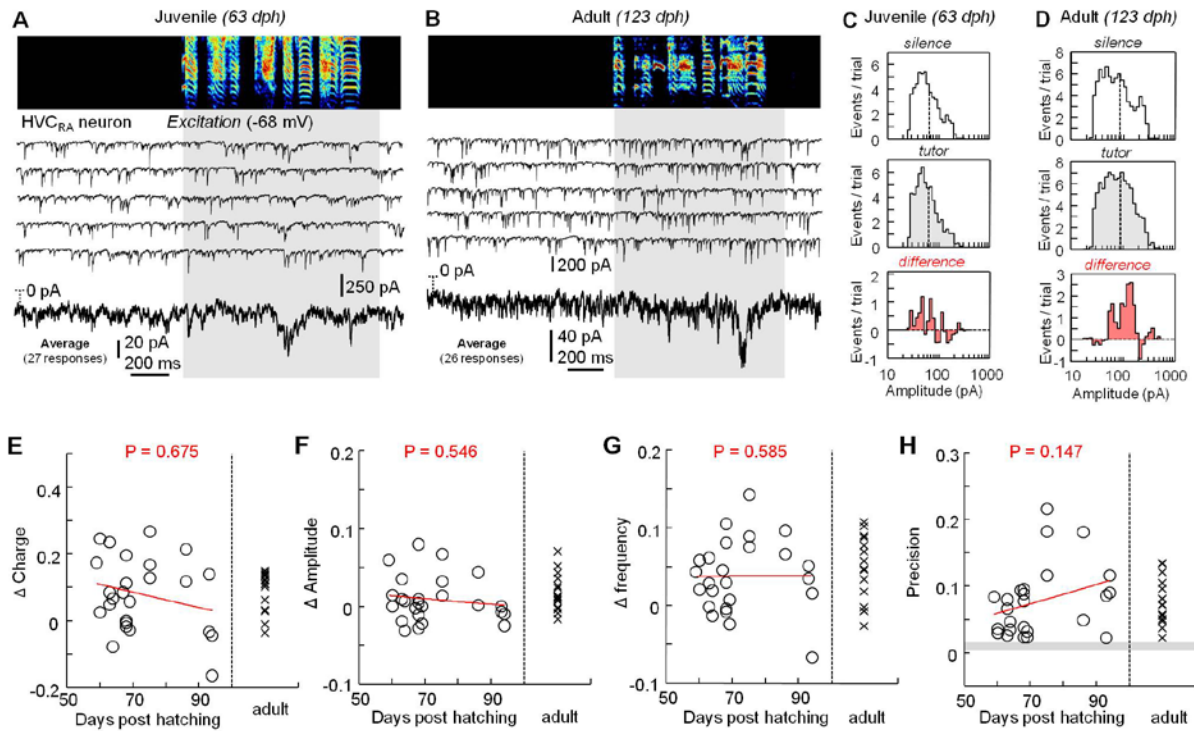


**Fig. S3. Tutor song-evoked excitatory synaptic currents in HVC premotor neurons.** (A and B) Five trials showing excitatory synaptic currents (holding potential: -68 mV) recorded in HVC premotor neurons during silence and tutor song presentation in a juvenile (A) and adult (B) zebra finch. Sonogram shown at top, and averaged trace given below. (C and D) Amplitude histograms of detected excitatory events during tutor song exposure and a 750 ms silent period for the premotor neurons shown in (A) and (B) respectively. At bottom is the difference between the number of detected events during silence and tutor song playback. (E to H) Throughout juvenile development, no age-related changes were observed in tutor song-evoked excitatory synaptic charge (E), the amplitude (F) and frequency (G) of excitatory events, and the precision of excitation across trials (H) ( $P > 0.15$ , linear mixed-effect model) (shaded region = 95% confidence interval). For all measures, a Pearson linear correlation was used to establish significance.

**Fig. S4**

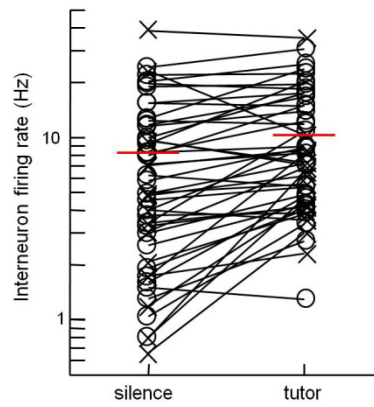


**Fig. S4. HVC interneuron spiking activity.** Firing rate of HVC interneurons across all birds during tutor song playback ( $10.4 \pm 8.4$  Hz) compared with a silent baseline period ( $8.2 \pm 8.3$  Hz) ( $P < 0.001$ , repeated measures ANOVA). The 'X's represent data taken from adults and 'O's represent data from juveniles (dph < 90). The y-axis has a logarithmic scale.

**Fig. S5**

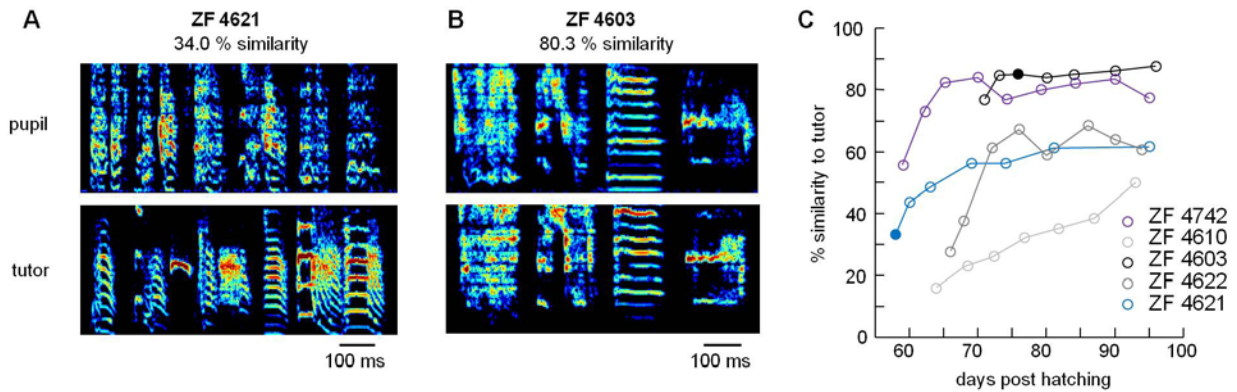


**Fig. S5. Learning trajectories of juvenile zebra finches.** (A) Example motif produced by the juvenile pupil ZF 4621 at 59 days posthatch, which has a 34% similarity to the tutor song (below). (B) Example motif produced by the juvenile pupil ZF 4603 at 76 days posthatch, which has an 80.3% similarity to the tutor song (below). (C) Learning trajectories for five of the zebra finches recorded as part of our study. Filled circles represent examples shown on the left.



**Fig. S7**

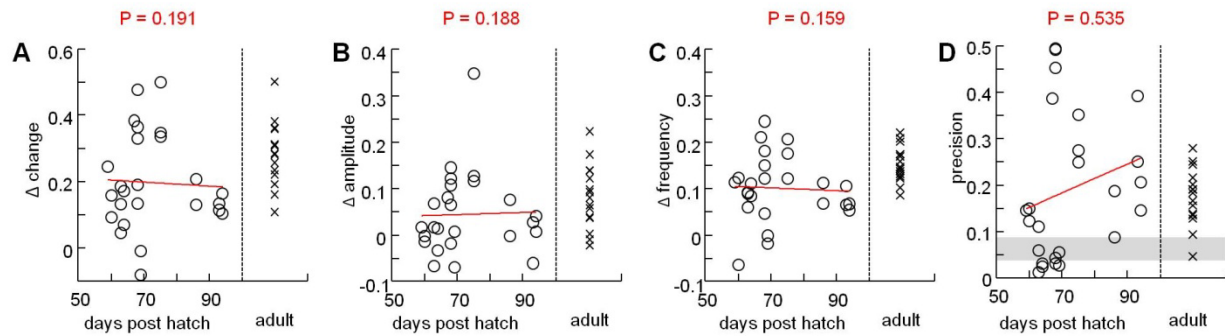


**Fig. S7. Inhibition induced by the tutor song is not dependent on age.** (A to D) Throughout juvenile development, no age-related changes were observed in tutor song-evoked inhibitory synaptic charge (A), the amplitude (B) and frequency (C) of inhibitory events, and the precision of inhibition across trials (D) (shaded region = 95% confidence interval). For all measures, a linear mixed-effect model was fitted to establish significance ( $P > 0.158$ )

**Fig. S8**

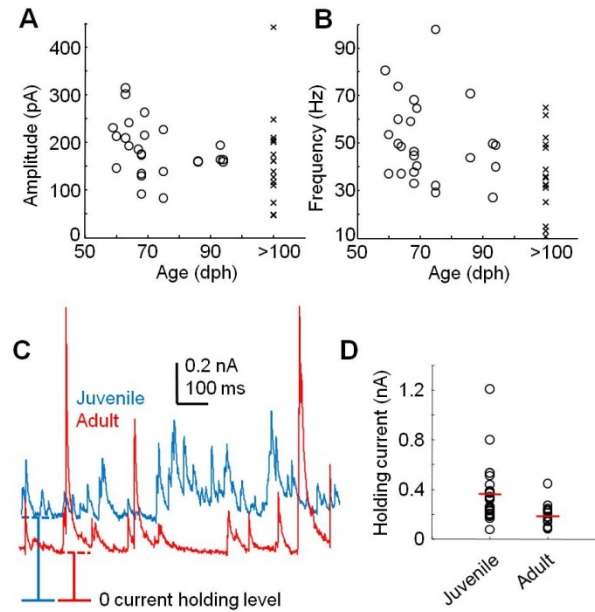


**Fig. S8. Sustained inhibition decreases with developmental age.** (A and B) Spontaneous inhibitory event amplitudes (A) and frequencies (B) in HVC premotor neurons did not differ with age ( $P > 0.2$ , linear mixed-effect model). (C) Example voltage clamp recordings of inhibitory currents of HVC premotor neurons during silence in a juvenile (blue) and an adult (red) bird. (D) Average holding current during silence of all juvenile ( $n = 25$  neurons) and adult ( $n = 15$  neurons) neurons recorded in voltage clamp in this study ( $P < 0.001$ , Wilcoxon rank sum test).

**Fig. S9**

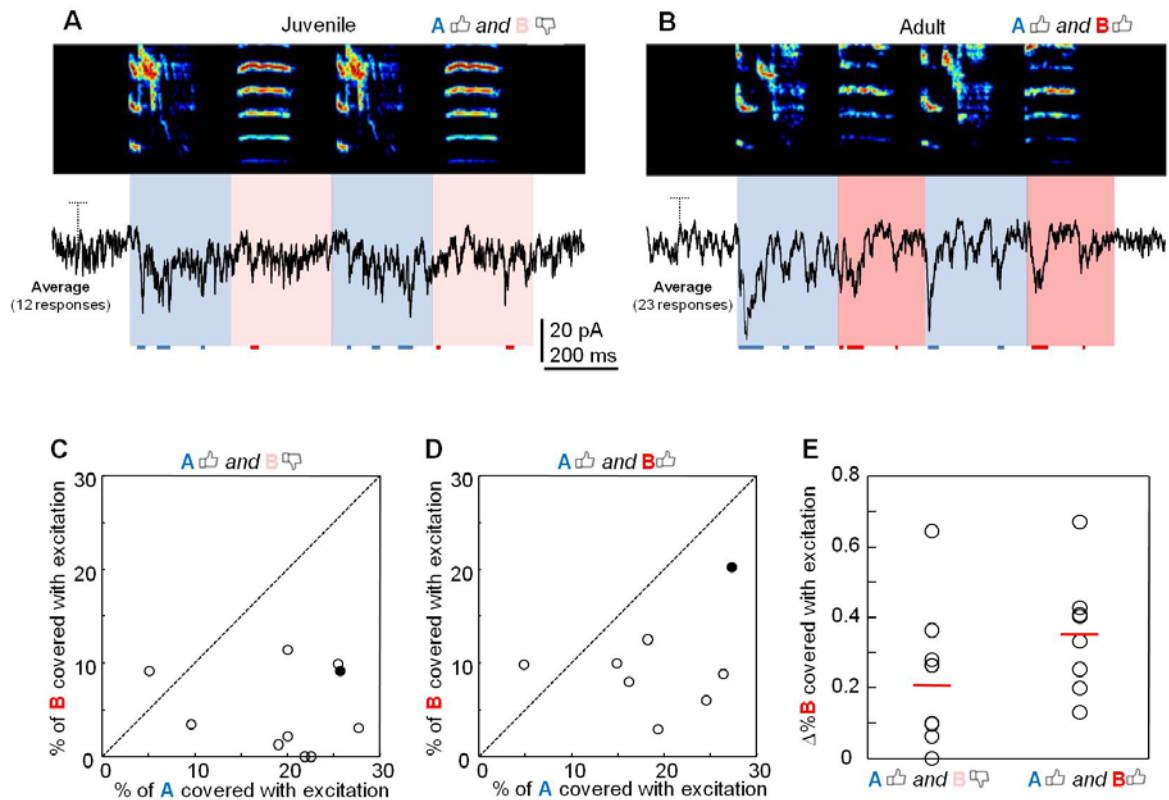


**Fig. S9. Synaptic excitation onto HVC premotor neurons evoked by synthetic tutor song presentation.** (A and B) Average excitatory current trace evoked by the synthetic tutor song 'ABAB' in a juvenile zebra finch performing a good copy of 'A' (76.9% similarity) and a poor copy of 'B' (49.6% similarity) (A) and in an adult zebra finch performing good copies of 'A' (85.3% similarity) and 'B' (87.9% similarity) (B). The red and blue horizontal lines represent periods in which the mean excitatory current onto HVC premotor neurons exceeds a 95% confidence interval. (C) Percentage of syllable 'A' and 'B' covered with significant excitation in juveniles imitating 'A' well and producing a poor copy of 'B'. Filled circles represent example traces. (D) Percentage of syllable 'A' and 'B' covered with significant excitation in adults performing a good copy of 'A' and 'B'. (E) Relative percentage of syllable 'B' covered by excitation did not significantly change from the early ( $0.21 \pm 0.20$ ) to the late ( $0.35 \pm 0.16$ ) learning phase ( $P = 0.081$ , Wilcoxon rank sum test).

**Fig. S10**

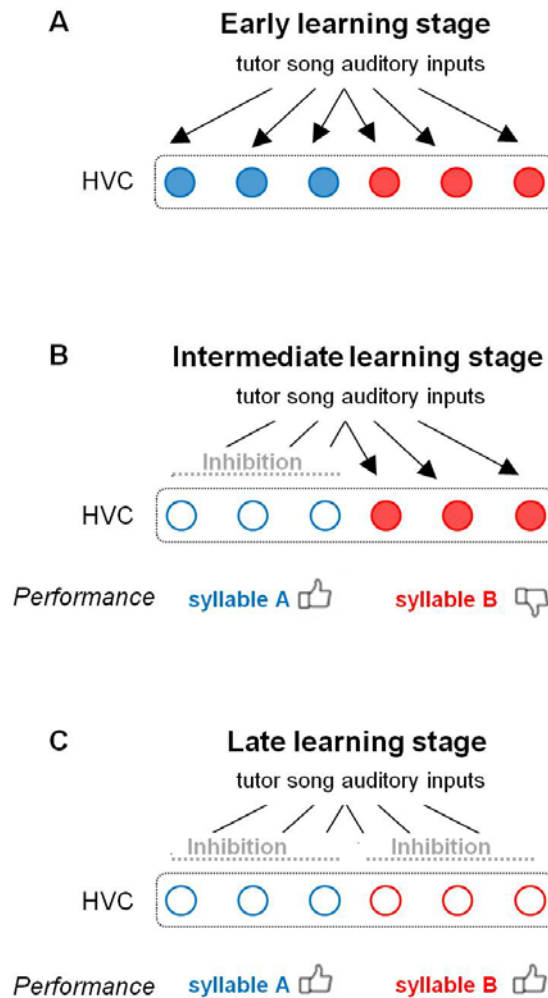


**Fig. S10. Model for neural mechanisms underlying sensorimotor integration during HVC circuit development.** (A) In initial stages of learning, auditory inputs are capable of driving HVC activity directly. Filled circles indicate that neurons are firing in response to the tutor song. (B) Once the bird has learned specific song elements (e.g. syllable ‘A’), HVC premotor neurons are selectively inhibited when observing that aspect of the tutor song. (C) After the song has been learned completely, inhibition shields HVC premotor neurons from the impact of the tutor song.

**Supplementary Movie:**

An adult zebra finch tutor (right) interacting with a juvenile. During this session, many repeated song motifs are presented to the juvenile bird.

**Additional Author notes:**

**Author contributions:** D.V., G.K., and M.A.L. designed the research; D.V., G.K., and D.L. performed the research; D.V., G.K., D.L., and M.A.L. analyzed the data, D.L. contributed reagents/analytic tools, and D.V., G.K., and M.A.L. wrote the paper.

## References

1. Y. Blandin, L. Lhuisset, L. Proteau, Cognitive processes underlying observational learning of motor skills. *Q. J. Exp. Psychol. A* **52**, 957–979 (1999). [doi:10.1080/713755856](https://doi.org/10.1080/713755856)
2. G. Fiorito, P. Scotto, Observational learning in *Octopus vulgaris*. *Science* **256**, 545–547 (1992). [Medline doi:10.1126/science.256.5056.545](https://pubmed.ncbi.nlm.nih.gov/1126/science.256.5056.545/)
3. A. Whiten, Imitation of the sequential structure of actions by chimpanzees (*Pan troglodytes*). *J. Comp. Psychol.* **112**, 270–281 (1998). [Medline doi:10.1037/0735-7036.112.3.270](https://pubmed.ncbi.nlm.nih.gov/1037/0735-7036.112.3.270/)
4. B. Kenward, C. Rutz, A. A. S. Weir, A. Kacelnik, Development of tool use in New Caledonian crows: Inherited action patterns and social influences. *Anim. Behav.* **72**, 1329–1343 (2006). [doi:10.1016/j.anbehav.2006.04.007](https://doi.org/10.1016/j.anbehav.2006.04.007)
5. M. Konishi, The role of auditory feedback in the control of vocalization in the white-crowned sparrow. *Z. Tierpsychol.* **22**, 770–783 (1965). [Medline](https://pubmed.ncbi.nlm.nih.gov/1965/22/770-783/)
6. O. Tchernichovski, P. P. Mitra, T. Lints, F. Nottebohm, Dynamics of the vocal imitation process: How a zebra finch learns its song. *Science* **291**, 2564–2569 (2001). [Medline doi:10.1126/science.1058522](https://pubmed.ncbi.nlm.nih.gov/1126/science.1058522/)
7. P. Ravbar, D. Lipkind, L. C. Parra, O. Tchernichovski, Vocal exploration is locally regulated during song learning. *J. Neurosci.* **32**, 3422–3432 (2012). [Medline doi:10.1523/JNEUROSCI.3740-11.2012](https://pubmed.ncbi.nlm.nih.gov/1523/JNEUROSCI.3740-11.2012/)
8. P. H. Price, Developmental determinants of structure in zebra finch song. *J. Comp. Physiol. Psychol.* **93**, 260–277 (1979). [doi:10.1037/h0077553](https://doi.org/10.1037/h0077553)
9. K. Immelman, Song development in the zebra finch and other estrilidid finches. In *Bird Vocalizations*, R. A. Hinde, Ed. (Cambridge Univ. Press, 1969), pp. 61–74.
10. F. Nottebohm, D. B. Kelley, J. A. Paton, Connections of vocal control nuclei in the canary telencephalon. *J. Comp. Neurol.* **207**, 344–357 (1982). [Medline](https://pubmed.ncbi.nlm.nih.gov/1982/207/344-357/)
11. E. E. Bauer, M. J. Coleman, T. F. Roberts, A. Roy, J. F. Prather, R. Mooney, A synaptic basis for auditory-vocal integration in the songbird. *J. Neurosci.* **28**, 1509–1522 (2008). [Medline doi:10.1523/JNEUROSCI.3838-07.2008](https://pubmed.ncbi.nlm.nih.gov/1523/JNEUROSCI.3838-07.2008/)

12. E. Akutagawa, M. Konishi, New brain pathways found in the vocal control system of a songbird. *J. Comp. Neurol.* **518**, 3086–3100 (2010). [Medline](#) [doi:10.1002/cne.22383](https://doi.org/10.1002/cne.22383)
13. E. T. Vu, M. E. Mazurek, Y. C. Kuo, Identification of a forebrain motor programming network for the learned song of zebra finches. *J. Neurosci.* **14**, 6924–6934 (1994). [Medline](#)
14. M. A. Long, M. S. Fee, Using temperature to analyse temporal dynamics in the songbird motor pathway. *Nature* **456**, 189–194 (2008). [Medline](#) [doi:10.1038/nature07448](https://doi.org/10.1038/nature07448)
15. D. Aronov, A. S. Andalman, M. S. Fee, A specialized forebrain circuit for vocal babbling in the juvenile songbird. *Science* **320**, 630–634 (2008). [Medline](#) [doi:10.1126/science.1155140](https://doi.org/10.1126/science.1155140)
16. T. F. Roberts, K. A. Tschida, M. E. Klein, R. Mooney, Rapid spine stabilization and synaptic enhancement at the onset of behavioural learning. *Nature* **463**, 948–952 (2010). [Medline](#) [doi:10.1038/nature08759](https://doi.org/10.1038/nature08759)
17. T. F. Roberts, S. M. Gobes, M. Murugan, B. P. Ölveczky, R. Mooney, Motor circuits are required to encode a sensory model for imitative learning. *Nat. Neurosci.* **15**, 1454–1459 (2012). [Medline](#) [doi:10.1038/nn.3206](https://doi.org/10.1038/nn.3206)
18. T. A. Nick, M. Konishi, Neural song preference during vocal learning in the zebra finch depends on age and state. *J. Neurobiol.* **62**, 231–242 (2005). [Medline](#) [doi:10.1002/neu.20087](https://doi.org/10.1002/neu.20087)
19. R. Mooney, Different subthreshold mechanisms underlie song selectivity in identified HVC neurons of the zebra finch. *J. Neurosci.* **20**, 5420–5436 (2000). [Medline](#)
20. D. Accorsi-Mendonça, R. M. Leão, J. F. Aguiar, W. A. Varanda, B. H. Machado, Urethane inhibits the GABAergic neurotransmission in the nucleus of the solitary tract of rat brain stem slices. *Am. J. Physiol. Regul. Integr. Comp. Physiol.* **292**, R396–R402 (2007). [Medline](#) [doi:10.1152/ajpregu.00776.2005](https://doi.org/10.1152/ajpregu.00776.2005)
21. S. Scotto-Lomassese, C. Rochefort, A. Nshdejan, C. Scharff, HVC interneurons are not renewed in adult male zebra finches. *Eur. J. Neurosci.* **25**, 1663–1668 (2007). [Medline](#) [doi:10.1111/j.1460-9568.2007.05418.x](https://doi.org/10.1111/j.1460-9568.2007.05418.x)

22. P. L. Rauske, S. D. Shea, D. Margoliash, State and neuronal class-dependent reconfiguration in the avian song system. *J. Neurophysiol.* **89**, 1688–1701 (2003). [Medline](#)  
[doi:10.1152/jn.00655.2002](https://doi.org/10.1152/jn.00655.2002)
23. J. N. Raksin, C. M. Glaze, S. Smith, M. F. Schmidt, Linear and nonlinear auditory response properties of interneurons in a high-order avian vocal motor nucleus during wakefulness. *J. Neurophysiol.* **107**, 2185–2201 (2012). [Medline](#) [doi:10.1152/jn.01003.2009](https://doi.org/10.1152/jn.01003.2009)
24. G. Kosche, D. Vallentin, M. A. Long, Interplay of inhibition and excitation shapes a premotor neural sequence. *J. Neurosci.* **35**, 1217–1227 (2015). [Medline](#)  
[doi:10.1523/JNEUROSCI.4346-14.2015](https://doi.org/10.1523/JNEUROSCI.4346-14.2015)
25. R. Mooney, J. F. Prather, The HVC microcircuit: The synaptic basis for interactions between song motor and vocal plasticity pathways. *J. Neurosci.* **25**, 1952–1964 (2005). [Medline](#)  
[doi:10.1523/JNEUROSCI.3726-04.2005](https://doi.org/10.1523/JNEUROSCI.3726-04.2005)
26. D. Lipkind, O. Tchernichovski, Quantification of developmental birdsong learning from the subsyllabic scale to cultural evolution. *Proc. Natl. Acad. Sci. U.S.A.* **108** (suppl. 3), 15572–15579 (2011). [Medline](#) [doi:10.1073/pnas.1012941108](https://doi.org/10.1073/pnas.1012941108)
27. G. Rizzolatti, L. Craighero, The mirror-neuron system. *Annu. Rev. Neurosci.* **27**, 169–192 (2004). [Medline](#) [doi:10.1146/annurev.neuro.27.070203.144230](https://doi.org/10.1146/annurev.neuro.27.070203.144230)
28. J. F. Prather, S. Peters, S. Nowicki, R. Mooney, Precise auditory-vocal mirroring in neurons for learned vocal communication. *Nature* **451**, 305–310 (2008). [Medline](#)  
[doi:10.1038/nature06492](https://doi.org/10.1038/nature06492)
29. T. K. Hensch, Critical period regulation. *Annu. Rev. Neurosci.* **27**, 549–579 (2004). [Medline](#)  
[doi:10.1146/annurev.neuro.27.070203.144327](https://doi.org/10.1146/annurev.neuro.27.070203.144327)
30. B. Morales, S. Y. Choi, A. Kirkwood, Dark rearing alters the development of GABAergic transmission in visual cortex. *J. Neurosci.* **22**, 8084–8090 (2002). [Medline](#)
31. Y. T. Li, W. P. Ma, C. J. Pan, L. I. Zhang, H. W. Tao, Broadening of cortical inhibition mediates developmental sharpening of orientation selectivity. *J. Neurosci.* **32**, 3981–3991 (2012). [Medline](#) [doi:10.1523/JNEUROSCI.5514-11.2012](https://doi.org/10.1523/JNEUROSCI.5514-11.2012)

32. M. Pecka, Y. Han, E. Sader, T. D. Mrsic-Flogel, Experience-dependent specialization of receptive field surround for selective coding of natural scenes. *Neuron* **84**, 457–469 (2014). [Medline doi:10.1016/j.neuron.2014.09.010](#)
33. D. G. Southwell, R. C. Froemke, A. Alvarez-Buylla, M. P. Stryker, S. P. Gandhi, Cortical plasticity induced by inhibitory neuron transplantation. *Science* **327**, 1145–1148 (2010). [Medline doi:10.1126/science.1183962](#)
34. R. H. Hahnloser, A. A. Kozhevnikov, M. S. Fee, An ultra-sparse code underlies the generation of neural sequences in a songbird. *Nature* **419**, 65–70 (2002). [Medline doi:10.1038/nature00974](#)
35. T. A. Pologruto, B. L. Sabatini, K. Svoboda, ScanImage: Flexible software for operating laser scanning microscopes. *Biomed. Eng. Online* **2**, 13 (2003). [Medline doi:10.1186/1475-925X-2-13](#)
36. S. Komai, W. Denk, P. Osten, M. Brecht, T. W. Margrie, Two-photon targeted patching (TPTP) in vivo. *Nat. Protoc.* **1**, 647–652 (2006). [Medline doi:10.1038/nprot.2006.100](#)
37. K. Kitamura, B. Judkewitz, M. Kano, W. Denk, M. Häusser, Targeted patch-clamp recordings and single-cell electroporation of unlabeled neurons in vivo. *Nat. Methods* **5**, 61–67 (2008). [Medline doi:10.1038/nmeth1150](#)
38. O. Tchernichovski, F. Nottebohm, C. E. Ho, B. Pesaran, P. P. Mitra, A procedure for an automated measurement of song similarity. *Anim. Behav.* **59**, 1167–1176 (2000). [Medline doi:10.1006/anbe.1999.1416](#)
39. D. Margoliash, Acoustic parameters underlying the responses of song-specific neurons in the white-crowned sparrow. *J. Neurosci.* **3**, 1039–1057 (1983). [Medline](#)